

https://doi.org/10.1070/QEL16187

Single-frequency TEA CO_2 laser with a bleaching spectral intracavity filter

V.R. Sorochenko

Abstract. **The regime of single-frequency operation is realised in a TEA CO_2 laser with a spectral filter inside the cavity (a cell filled with SF_6) on P(12)–P(24) lines of the 10P band. The minimal scatter of the peak powers of the laser pulses in a series of 'shots' and the maximal ratio of the output energies in the single-frequency and free running regimes (greater than 0.84) are obtained on the P(16) line at an optimal SF_6 pressure in the cell. Experimental results qualitatively agree with the absorption spectrum of SF_6 calculated from the SPECTRA information-analytical system. It is shown that the high ratio of energies in two regimes is achived due to gas bleaching in the cell.**

Keywords: *CO_2 laser, longitudinal cavity mode, single-frequency regime, SF_6.*

1. Introduction

Experiments on interaction of radiation of a pulsed CO_2 laser with matter require high reproducibility of the peak radiation power from 'shot' to 'shot'. In the case of a TEA CO_2 laser with a gas mixture pressure of $p \leqslant 1$ atm, operating at the fundamental transverse mode TEM_{00} of the cavity with a typical length of $L = 1–2$ m, several longitudinal modes participate in free running (FR) lasing, which have the frequencies close to the centre frequency of the rotational–vibrational transition involved in lasing. Self-mode-locking in the laser active medium results in that the time profile of the radiation pulse comprises several superimposed low-contrast pulse trains [1]. Pulses in the trains have a period of $\Delta T_0 = 2L/c$. In this case, both the pulse profile in trains, and the pulse contrast vary from shot to shot, which leads to multiple variations of the output peak power even if the output energy is stable (the spread of the output energy for well known commercial TEA CO_2 lasers is at most 10%).

To stabilise the peak radiation power, it is necessary to select a single longitudinal mode among several modes participating in lasing; in other words, single-frequency generation (SFG) should be provided, which is characterised by a smooth temporal profile of the laser pulse. Selection of longitudinal modes in the cavity of a TEA CO_2 laser is most frequently realised using the following methods [2]: 1) selective amplification of radiation inside the cavity in a frequency band having the width close to the frequency interval between neighbouring longitudinal modes $\Delta\nu_{long} = c/(2L)$ (hybrid CO_2 lasers comprising high- and low-pressure sections in the same cavity); 2) injecting radiation of stabilised a cw CO_2 laser into the cavity of a pulsed laser, which results in lasing in a longitudinal mode with the nearest frequency; 3) ensuring a high Q-factor for the cavity in the frequency band width $\sim\Delta\nu_{long}$ by employing intracavity interferometers; 4) embedding spectral filters into the cavity, i.e., elements, which have an absorption spectrum (AS) possessing narrow dips comparable in width to the value of $\Delta\nu_{long}$.

The latter approach seems the most simple from the technical point of view. However, it has an obvious drawback. Since gases are used as spectral filters, their absorption spectra may limit the number of CO_2-laser lines on which SFG may occur when the cell is filled with a particular gas. For example, sulphur hexafluoride (SF_6), which is the most frequently used as a filter, possesses absorption only in the central part of the 10P spectral band of the CO_2 molecule rotational–vibrational transitions [lines P(12)–P(24)]. For SFG in TEA CO_2 lasers in the bands 10R, 9P and 9R, other gases were used as spectral filters with the AS in the corresponding ranges [3–5]. However, in some problems concerning nonresonant interaction of radiation with matter, a change in the radiation wavelength within the limits of the CO_2-laser generation spectrum weakly affects the result obtained and is not a substantial problem.

For the first time, operation of a TEA CO_2 laser on a single longitudinal mode with an intracavity cell filled with SF_6 at a pressure of 0.5 Torr was observed in [6] where the cavity diffraction grating was adjusted to the 10P(18) line. This kind of selector was more thoroughly studied in [7, 8]. In [8], a 10-cm-long cell with the SF_6 pressure $p_{SF_6} < 1$ Torr was placed inside a cavity and SFG was realised on the P(14)–P(22) lines. Radiation of an auxiliary cw tunable CO_2 laser was matched with centres of the lines, and the frequency shift $\delta\nu$ between the pulsed and cw radiation was measured by using a scanning Fabry–Perot interferometer. A comparison of $\delta\nu$ for each of the lines with the SF_6 molecule AS structures from [9] near line centres has revealed that the frequencies of pulsed radiation exactly fit the minima in the AS, i.e, the SFG obtained is the result of spectral selection. The best pulse-to-pulse reproducibility of the SFG regime at $\Delta\nu_{long} = 61.2$ MHz was observed in [8] on the lines P(14), P(16) and P(22). On the lines P(18) and P(20), a multi-frequency regime was realised in some shots; in the SFG regime, the radiation frequency spasmodically (by several hundred MHz) changed from shot to shot.

In further works [10, 11], the SFG regime was obtained in TEA CO_2 lasers with a high peak power of the radiation

V.R. Sorochenko A.M. Prokhorov General Physics Institute, Russian Academy of Sciences, ul. Vavilova 38, 119991 Moscow, Russia; e-mail: soroch@kapella.gpi.ru

Received 1 August 2016; revision received 2 November 2016
Kvantovaya Elektronika **47** (1) 20–25 (2017)
Translated by N.A. Raspopov

pulse (up to 14 MW) on several lines of the 10P band at the cell length of 2 mm and pressure $p_{SF_6} \approx 5$ Torr; however, it has not been studied thoroughly. In [12], the SFG regime was obtained in a TEA CO_2 laser with a selective ring cavity, which comprised a 10-cm-long cell with SF_6 (the value of p_{SF_6} was not specified in [12]) and was adjusted to the 10P(16) line.

Despite the obvious physical mechanism of SFG in TEA CO_2 lasers with an intracavity cell filled with SF_6, there are rather important questions concerning practical employment of this method in a particular laser. These are: what is the reason for different stability of the SFG regime on different lines of the 10P band, which has been observed in [8]? is it possible to realise the spread of peak radiation powers in a shot series in the SFG regime that would be comparable to the energy spread in the FR regime? how much of the laser radiation pulse energy falls in transferring from FR to SFG?

The present work is aimed at answering these questions by the example of a particular TEA CO_2 laser [13]. Also, we for the first time studied SFG on the lines P(12) and P(24), i.e., in the whole absorption range of SF_6 near $\lambda = 10$ μm.

2. Experimental setup

A TEA CO_2 laser was used with the self-sustained discharge occupying a domain of size 1×1×30 cm, which was pumped by a two-stage Fitch pulsed voltage generator with step capacitances of 20 nF. A RU-65 discharger used as a switch element, and the charge voltage was $U_{charg} = 18-23$ kV. Two-side UV pre-ionisation of the discharge gap was provided by a sectioned surface spark discharge. The working mixture composition was $CO_2:N_2:He = 40:40:20$ at atmospheric pressure.

The optical schematic diagram of the installation is shown in Fig. 1. A three-mirror selective cavity of the laser with a length $L = 140$ cm ($\Delta\nu_{long} = 107$ MHz, $\Delta T_0 = 9.3$ ns) was formed by an output wedge germanium mirror M1 with a reflection coefficient of 60%, an aluminium diffraction grating (DG) 100 lines mm^{-1} and a concave highly reflecting mirror M2 with the radius of curvature $R = 3$ m. Mirror M1 and a unit with a NaCl window were mounted to flanges of the laser discharge chamber. The concave mirror could move along the cavity axis within several millimetres at an accuracy of 1 μm. An intracavity diaphragm 8 mm in diameter arranged near the highly reflecting mirror was used for selecting transverse modes. The Gaussian transverse distribution of the laser output radiation power confirms that lasing occurs on the fundamental transverse cavity mode TEM_{00} [13]. A cylindrical cell with an aperture of 30 mm and NaCl windows was filled with SF_6 and placed inside the cavity. To reduce radiation losses to Fresnel reflection, the cell was arranged in such a way that its axis was inclined at an angle of 45° to the cavity axis. The optical path length inside the cavity was 17 mm. All laser elements were arranged on an optical table made of synthetic granite (Eksma, Vilnius).

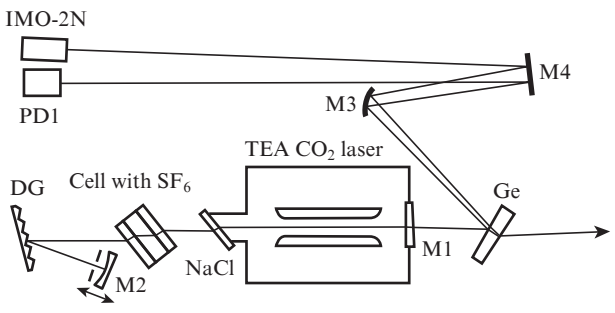

Figure 1. Optical scheme of the setup.

At the laser output, a splitting germanium wedge plate with a transmittance of 50% was placed. The beams reflected from its front and rear faces were directed by a concave mirror M3 with a curvature radius $R = 6$ m and a plane mirror M4 to a photodetector PD1 and energy meter IMO-2N (the accuracy is ±7%) (Fig. 1). The signal from PD1 passes to a digital Tektronix TDS 3052 oscilloscope with the bandwidth of 500 MHz and sampling rate of 5×10^9 s^{-1}. In this way, both the energy and the temporal profile of the laser pulse could be recorded in each shot. Typical oscillograms of laser radiation pulses are shown in Fig. 2 for FR and SF regimes (it is the same pulse in Figs 2a and 2b) on the 10P(22) line. The FWHM pulse duration is ~80 ns.

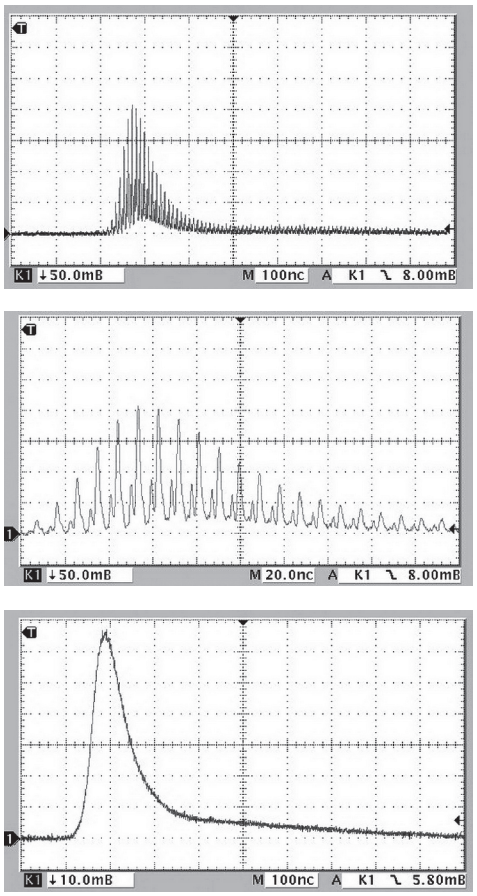

Figure 2. Oscillograms of the laser pulse [10P(22) line] in the (a, b) FR and (c) SFG regimes. The scales are (a, c) 100 ns div^{-1} and (b) 20 ns div^{-1}.

The maximum output energy in the FR regime on the most intensive line 10P(20) reached 40 mJ. In Fig. 3 one can see the laser radiation energy E in the FR regime measured behind the splitting plate as a function of the line number coinciding with the rotational quantum number J of the lower transition level, when the DG was adjusted to 10P band lines. Each point in Fig. 3 corresponds to the energy averaged over six laser shots.

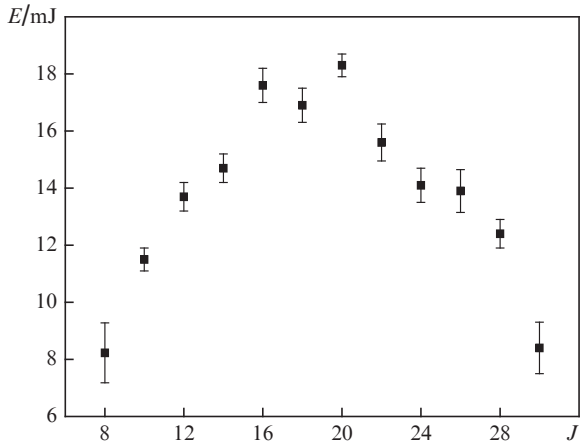

Figure 3. Laser pulse energy E in the FR regime vs. line number J.

3. Measurement results and discussion

3.1. SFG realised on various transitions of the 10P band of CO_2 molecule

SFG on the lines P(12)–P(24) of the CO_2-molecule 10P band was studied. For each line, the pressure of SF_6 in cell p_{SF_6} elevated stepwise (with the step of 1–2 mm controlled by an oil pressure gage, which corresponds to 0.064–0.13 Torr) starting from 0.2 Torr. For each value of p_{SF_6}, the cavity length was adjusted with a step of ~1 μm to minimise the depth of time profile modulation for radiation pulses due to beatings between several longitudinal modes. In this way, the minimal pressure $p_{SF_6}^{min}$ was found, at which the modulation depth of the radiation pulse was less than 2% (it was determined by the minimal detectable modulation amplitude on the oscilloscope screen) in a series of $n = 25$ shots (with a 1-minute interval between them) without additional adjustment of the cavity length L. In each shot, the time profile of the radiation pulse, its amplitude U_1, and energy E_{SFG} measured in the beam reflected from the splitting plate were controlled. The measurements were taken at a fixed voltage $U_{charg} = 22$ kV, at which the energy of the radiation pulse in the FR regime was close to maximal. The number of shots in a series ($n = 25$) was chosen experimentally. At n noticeably less than 25 (~10), the scatter in parameters U_1 and E_{SFG} substantially (at most twice) varied from series to series; at $n > 25$ it negligibly (at most by 10%) increased with n. Shorter series ($n = 10$–12) were realised for each line with an evacuated cell (FR regime) as well. The values of n lower than in the SFG regime are explained by a substantially less spread of energy E_{FR} (it was below ±5% of an average value).

The minimal values $p_{SF_6}^{min}$ have been found for all lines except for the line P(24). In the latter case, even at $p_{SF_6} = 1.4$ Torr when the laser operated near the threshold, the maximal number of shots in a series was not greater than 12 in the SFG regime.

In Table 1, for each of the seven lines, the following output laser parameters are presented for $p_{SF_6} = p_{SF_6}^{min}$: $E_{SFG}/\bar{E}_{FR}$, where $\bar{E}_{FR}$ is the radiation energy in the FR regime averaged over a series; E^{max}/E^{min} and U_1^{max}/U_1^{min} are the maximal to minimal value ratios for the pulse energy and amplitude in a series in the SFG regime; and $\Delta\nu_{SFG}$ is the range of selected mode frequency (ν) variation, within which the SFG is realised (a change of L by 1 μm corresponds to variation of ν by 20 MHz).

Table 1.

J	$p_{SF_6}^{min}$/Torr	$E_{SFG}/\bar{E}_{FR}$	E^{max}/E^{min}	U_1^{max}/U_1^{min}	$\Delta\nu_{SFG}$/MHz
12	1.28	0.58–0.75	1.28	1.29	20
14	0.90	0.66–0.89	1.34	1.37	40
16	0.32	0.86–1.00	1.17	1.13	100
18	0.61	0.64–0.93	1.44	1.38	20
20	0.80	0.53–0.81	1.52	1.50	20
22	0.77	0.74–0.96	1.30	1.28	100
24	1.31	0.53–0.71	1.33	1.29	20

Measurements show that the maximal values of $E_{SFG}/\bar{E}_{FR}$ were observed on the line P(16), whereas the scatter in parameters E_{SFG} and U_1 was two–tree times less than on the other lines. For explaining the difference in spreads of these parameters we used the spectral dependence of the linear absorption coefficient $K(\nu)$ of SF_6 molecule calculated in the ranges close to line centres of the CO_2-molecule transitions mentioned above. The dependence was obtained by using the HITRAN database of the SPECTRA information-analytical system [14].

A fragment of the SF_6 absorption spectrum in the frequency range -650 MHz $< \nu < +650$ MHz (hereinafter, for a zero frequency we take the centre of the corresponding line; line frequency data are taken from [15]) is shown in Fig. 4a for the line 10P(16) at $p_{SF_6}^{min} = 0.32$ Torr. One can see that at $\nu = 136$ MHz the coefficient K takes the minimal value of

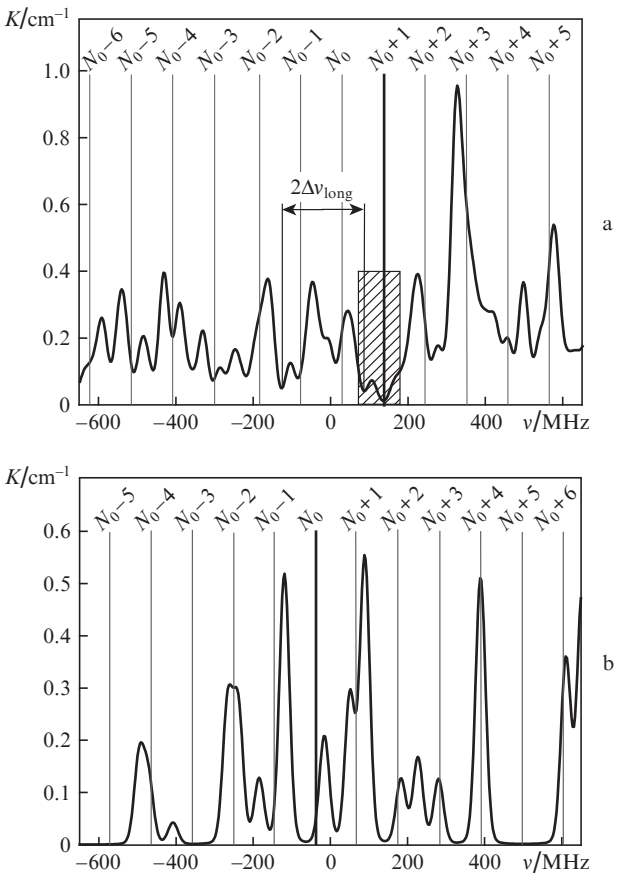

Figure 4. Fragments of the SF_6 linear absorption spectrum near centres of (a) 10P(16) and (b) 10P(20) lines at SF_6 pressures in the cell 0.32 and 0.8 Torr, respectively (data from the HITRAN database of the SPECTRA system [14]). For $\nu = 0$ is taken the centre frequency of the corresponding line (line frequencies are taken from [15]).

0.014 cm^{-1} within the limits of the specified frequency range. The value of K in other minima of the absorption spectrum is substantially greater. In addition, with a distance from $\nu = 0$, according to the Lorentzian profile of the laser transition gain, the small-signal gain falls, which also favours suppression of weak modes that are far from the line centre. Vertical lines in Fig. 4a mark the frequencies of longitudinal laser cavity modes that are optimal for selecting a single longitudinal mode. Here, to each mode corresponds the number N equal to the number of half-waves filling the cavity length; N_0 is the number of half-waves for the mode nearest to the line centre (in what follows, we will characterise each longitudinal mode by its number: mode N_0, mode $N_0 + 1$, etc.). From Fig. 4a follows that the least losses correspond to the mode $N_0 + 1$ with a frequency $\nu_{opt} = 136$ MHz (marked by a heavy line). A longitudinal mode with the frequency fitting the hatched range will have losses less than all other modes within the limits of the spectrum from Fig. 4a. Actually, the width of this range is $\Delta\nu_{long} = 107$ MHz. In experiments, at $p_{SF_6} \geqslant p_{SF_6}^{min}$, the SFG regime was realised almost in the same range of ν variations ($\Delta\nu_{SFG} \approx 100$ MHz). Only at boundaries of this region, the pulse top was modulated with the periods ΔT_0 or $\Delta T_0/2$ and depths of up to 3.8% or 2.6%, respectively, due to the second longitudinal mode. This corresponds to the case where the frequencies of modes $N_0 + 1$ and $N_0 + 2$ are close to the boundaries of the hatched range (the period ΔT_0) or when the frequencies of modes $N_0 - 1$ and $N_0 + 1$ are close to two minima separated by the interval $2\Delta\nu_{long}$ (period $\Delta T_0/2$).

The study of the spectrum $K(\nu)$ near centres of other lines pertaining to the 10P band yields that the possibility of selecting a single longitudinal mode for each line substantially depends on a particular value of L. Consider an example of the P(20) line. The fragment of the spectrum $K(\nu)$ near the centre of the P(20) line is shown in Fig. 4b in the same frequency range as in Fig. 4a, and the frequencies of longitudinal modes are specified at which the mode N_0 (marked by a heavy line) has the least, however, non-zero losses among the nearest modes. In our case, the selection regime for the P(20) line is very unstable because under a small (by ~10 MHz) shift to the right of the N_0 mode frequency, the increase in its amplitude per pass through the amplifier–cell system may become equal to the corresponding parameter for modes $N_0 + 5$ and $N_0 - 3$ (for which $K \approx 0$, but the gain in the laser active medium is noticeably less). Correspondingly, at a small (by ~10 MHz) frequency shift to the left, the mode $N_0 - 1$ may also participate in lasing; at a large frequency shift (by ~25 MHz), the mode $N_0 + 2$ may be involved. In the experiment, at small detuning of L from the optimal value L_{opt} (SFG regime requires that L be adjusted with an accuracy of 1 μm), the time profile of the radiation pulse in different shots was modulated with the periods ΔT_0, $\Delta T_0/3$, $\Delta T_0/8$ and depth of up to 7%, 2.7% and 9.5%, respectively. This confirms that the laser radiation spectrum comprises the modes mentioned above, which compete with the mode N_0. Absence of modulation with a period $\Delta T_0/2$ confirms passive stability of the cavity within 1 μm. Judging from the very large spread of the parameters U_1 and E_{SFG} from shot to shot in the SFG regime, one may assume that even at $L = L_{opt}$ the number N (or the frequency) of the selected mode can spasmodically change. Large variations in E_{SFG} and U_1 are related with that lasing in the modes with $|N - N_0| = 3–5$ occurs at a smaller, that in the nearest to N_0 modes, gain but at K_0, whereas lasing in nearest to N_0 modes with the initial absorption in SF_6 is accompanied by medium bleaching at the instant of the radiation pulse formation (see below Sect. 3.2.). A similar effect, though at $L = 2.45$ m, was observed in [8], where the frequency shift of the selected mode relative to $\nu = 0$ in the case of the P(20) line in particular shots was $\delta\nu = -300$, -100, and +500 MHz. Note that, taking into account the measurement error of ±25 MHz, these values of $\delta\nu$ correspond to the absorption minima in Fig. 4b. This testifies that the spectrum fragment $K(\nu)$ in Fig. 4b qualitatively explains the results of our experiment and of work [8].

Fragments of the SF_6 absorption spectrum $K(\nu)$ near centres of lines P(12), P(14), P(18), P(22) and P(24), obviously, substantially differ from Fig. 4b. However, there is a common feature: in the frequency interval -650 MHz $< \nu <$ +650 MHz there are many ranges where $K \approx 0$. At a prescribed value of L (that is, $\Delta\nu_{long}$), such a structure of $K(\nu)$ will help one to select longitudinal modes with various numbers N. Sometimes, as in the case of the line P(20), the value of $|N - N_0|$ may reach 5. If the cavity length L is not stabilised (to an accuracy of ~0.1 μm), then at small $\Delta\nu_{SFG}$ the value of N may jump from shot to shot due to a thermal shift of L, i.e., the laser frequency ν may vary, which results in large variations of E_{SFG} and U_1 similarly to the line P(20). However, a large scatter of the parameters E_{SFG} and U_1 may also occur in selecting a longitudinal mode with a particular N value in the case where absorption peaks have a large slope $dK/d\nu$ in a certain segment of the spectrum (see Section 3.2.). The value of $\Delta\nu_{SFG}$ for various lines is determined by the possibility of lasing in several longitudinal modes that have close increments of radiation power rise, which directly depends on a particular profile of the curve $K(\nu)$ and on the value of L.

Thus, the investigation performed has revealed advantages of SFG on the line P(16) in our laser. In practical realisation of SFG regime it is important to know not only the value of $p_{SF_6}^{min}$ but also the pressure range $p_{SF_6}^{opt}$ for this line, within which the radiation parameters vary weakly. This pressure range will help one to determine an adequate method for SF_6 puffing and controling its pressure in the cell. This will be considered in Section 3.2.

3.2. Optimal range of the SF_6 pressure for the P(16) line. Cell bleaching

In measurements, the pressure of SF_6 in the cell was 0.32, 0.42 and 0.51 Torr (5, 6.5 and 8.0 mm by the oil pressure gage). Similarly to Section 3.1, measurements were taken at a fixed voltage $U_{charg} = 22$ kV. Measurement results are presented in Table 2. In addition to the parameters from Table 1, the following parameters are presented: $\overline{\Delta t_1}$ is the delay of the laser radiation pulse maximum relative to the pump pulse onset Δt_1, averaged over a shot series; $\Delta t_2 = (\overline{\Delta t_1})_{SFG} - (\overline{\Delta t_1})_{FR}$ is the time shift between the maxima of the pulses in the SFG and FR regimes averaged over a pulse series. Measurements at $p_{SF_6} = 0.32$ and 0.42 Torr show that E^{max}/E^{min} and U_1^{max}/U_1^{min} increase moderately with a rise of the pressure p_{SF_6}; however, at $p_{SF_6} = 0.51$ Torr the increase is noticeable. From this follows that in order to obtain not only smooth radiation pulses reproducible in each shot but also the minimal spread of the values E_{SFG} and U_1 in a shot series, the pressure p_{SF_6} should be chosen from a certain interval; in our case, it is $p_{SF_6}^{opt} = 0.32–0.42$ Torr.

The pressure $p_{SF_6}^{opt}$ depends on the gain per transit across the laser active medium: the higher the gain, the greater the SF_6 pressure should be taken, and vice versa. In a separate experiment we have realised stable SFG while simultaneously

Table 2.

p_{SF_6}/Torr	$\overline{\Delta t_1}$/ns	Δt_2/ns	E^{max}/E^{min}	U_1^{max}/U_1^{min}	$E_{SFG}/\bar{E}_{FR}$
0	650	0	1.094	–	–
0.32	850	200	1.17	1.13	0.86–1.00
0.42	960	310	1.19	1.14	0.84–0.99
0.51	1100	450	1.33	1.26	0.75–0.99

reducing U_{charg} and p_{SF_6}; however, the spread of pulse parameters was substantially greater than at p_{SF_6} = 0.32 Torr and U_{charg} = 22 kV because the laser operated near the threshold.

From Table 2 follows that at p_{SF_6} = 0.32 Torr we succeeded to reach the ratio $E_{SFG}/\bar{E}_{FR}$ = 0.86–1.00. Simultaneously, there is a noticeable (by 200 ns) increase in Δt_1 in the SFG regime due to absorption losses in SF_6. All these facts lead to assumption that gas undergoes bleaching in a cell. To additionally confirm this, we have performed a simple experiment. On the diaphragm in a laser cavity that was used for selecting the TEM_{00} mode we placed a 28-μm-thick film made of high-pressure polyethylene. Film transmission at the wavelength of the P(16) line was preliminarily measured (it was 0.89±0.01) and it was established that the film actually does not disturb the spatial intensity distribution of the laser beam. With a cavity comprising the film and evacuated cell, the delay in a series of 10 shots was $\overline{\Delta t_1}$ = 800 ns, and the radiation energy varied within the limits of 0.42–0.46 relative to the value of $\bar{E}_{FR}$ measured without the film inside the cavity. Obviously, if a thicker film made of the same material is used then, in order to increase $\overline{\Delta t_1}$ to 850 ns (as in the SFG at p_{SF_6} = 0.32 Torr), the radiation energy should be even lower (rough estimation yields the value less than $0.4\bar{E}_{FR}$). This effect would be expected in the SFG regime at p_{SF_6} = 0.32 Torr with absent bleaching.

In the domain where the cell with SF_6 is placed inside a cavity, the maximal radiation intensity corresponding to the energy density of 0.27 J cm^{-2} (the estimate from [13]) reached 2×10^6 W cm^{-2}. This value is above the saturation intensities estimated in [16] both for single-photon transitions between the fundamental and first vibrational levels of ν_3 mode in SF_6 molecule (less than 10^5 W cm^{-2}), and for two- and three-photon transitions to second and third vibrational levels (10^5–10^6 W cm^{-2}). The estimates were made for small values p_{SF_6} (that are on the order of those in the present work), when rotational and vibrational relaxations of the level population can be neglected during the first spike of the laser pulse. These relaxation times can be estimated as $p_{SF_6}\tau_{VV}$ = 50 ns Torr and $p_{SF_6}\tau_{RR}$ = 35 ns Torr. In this aspect, the situation with SF_6 at a sub-Torr pressure greatly differs from the case of using cells with an SF_6–He mixture (several Torr SF_6 and up to 10 atm He) for increasing the contrast of a short radiation pulse at $\lambda \approx 10$ μm, where the relaxation time of the bleached state may be ~1 ns [17, 18]. In the case of bleaching, the transmission of the gas inside the cell is directly related to the relaxation time of the bleached state. At pressures of SF_6 equal to a fraction of Torr the transmission may be close to 100%, whereas in the case described in [17, 18] it was conventionally at most 50%.

Reduction of the radiation pulse energy in the SFG regime as compared to the FR regime at p_{SF_6} = 0.32 Torr can be explained by that in our case the first spike of the radiation pulse is formed on the falling dependence of the small-signal active medium gain on time $\alpha(t)$ (the characteristic FWHM time is ~3 μs). The maximal value of $\alpha(t)$ is attained in ~100 ns after the pump pulse termination. The duration of the latter was ~200 ns. Hence, a small reduction of the value of α_0 [which is the value of $\alpha(t)$ at the instant of the pulse spike formation] that determines the radiation energy yields the energy difference for two regimes.

From Table 2, one can see that with an increase in p_{SF_6} the ratio $E_{SFG}/\bar{E}_{FR}$ falls. The reason is that $\overline{\Delta t_1}$ increases with increasing p_{SF_6}; hence, α_0 reduces. Obviously, the regime of absorber bleaching in this case is kept, and the parameter $E_{SFG}/\bar{E}_{FR}$ insignificantly falls. The greater scatter in parameters E_{SFG} and U_1 in a shot series in the case of rising p_{SF_6} can be explained by that, according to calculation with the help of the SPECTRA system, the slope dK/dν of the SF_6 absorption peak sides increases (hence, so does dK/dL) (Fig. 4a). The thermal shift of the cavity length dL between laser shots is the main reason of a greater spread of the values of E_{SFG} and U_1 as compared to the scatter in E_{FR} in a shot series.

Thus, the choice $p_{SF_6} = p_{SF_6}^{opt}$ = 0.32–0.42 Torr in the case of lasing on the P(16) line gives a chance to simultaneously realise the maximal stability of the peak radiation pulse power and its maximal energy. However, even at $p_{SF_6} = p_{SF_6}^{opt}$ the value of U_1^{max}/U_1^{min} was noticeably greater than E^{max}/E^{min} in the FR regime. For reducing it to the level of 9.4% reached in the FR regime, the cavity length should be stabilised with an accuracy of ~0.1 μm, which in the case of a TEA CO_2 laser is a sufficiently challenging technical problem. The solution of this problem will substantially reduce the scatter in the radiation parameters in cases of other lines of the 10P band.

4. Conclusions

Thus, the following results have been obtained in the present work:

1. The regime of SFG is realised on the P(12)–P(24) lines of the 10P band in a TEA CO_2 laser with a bleaching spectral filter (a 1.7-cm-long cell filled with SF_6 at a pressure of less than 1.4 Torr) in a selective cavity of length L = 1.4 m. The scatter in energy and peak radiation pulse powers in a shot series substantially depended on the line number, which is qualitatively explained by the absorption spectrum of SF_6 calculated from the SPECTRA information-analytical system.

2. The minimal (at most 14%) scatter in peak radiation pulse powers in a shot series was realised on the P(16) line with the pressure of SF_6 in cell from the optimal range 0.32–0.42 Torr. To reduce the energy spread to the level of 9.4% obtained in the FR regime, the cavity length should be stabilised to an accuracy of ~0.1 μm.

3. By choosing the pressure of SF_6 in the cell within the optimal range we succeeded to obtain the radiation pulse energy in the SFG regime on the P(16) line, which is above 84% of the energy in the FR regime. Close values of E_{SFG} and E_{FR} obtained in the case of initial radiation losses due to absorption in SF_6 confirm the fact of gas medium bleaching. A simple experiment showed that at p_{SF_6} = 0.32 Torr with absent bleaching, the energy E_{SFG} would be less than 40% of E_{FR}.

The results obtained in the present work may be useful in realising the single-frequency operation in TEA CO_2 lasers.

Acknowledgements. The author is grateful to colleagues from the A.M. Prokhorov General Physics Institute, S.Yu. Kazantsev, N.V. Pletnev and Yu.L. Kalachev, for help in equipping the experimental stand and useful discussions. The author also thanks the journal reviewer for useful remarks, which substantially improved the quality of the paper.

The work was initiated by projects of the Russian Foundation for Basic Research (Grant Nos 13-02-12181 and 15-59-31817).

References

1. Kovalev V.I. *Kvantovaya Elektron.*, **23**, 135 (1996) [*Quantum Electron.*, **26**, 131 (1996)].
2. Novgorodov M.Z., Chokoev E.S. *Trudy FIAN*, **221**, 139 (1992).
3. Dougal R.A., Jones C.R., Gundersen M.A., Nelson L.Y. *Appl. Opt.*, **18**, 1311 (1979).
4. Dougal R.A., Gundersen M.A., Williams P.F. *Rev. Sci. Instrum.*, **53**, 181 (1982).
5. Quack M., Ruede C., Seytang G. *Spectrochim. Acta, Part A*, **46**, 523 (1990).
6. Lyon D.L., George E.V., Haus H.A. *Appl. Phys. Lett.*, **17**, 474 (1970).
7. Nurmikko A., DeTemple T.A., Schwarz S.E. *Appl. Phys. Lett.*, **18**, 130 (1971).
8. DeTemple T.A., Nurmikko A. *Opt. Commun.*, **4**, 231 (1971).
9. Hinkley E.D. *Appl. Phys. Lett.*, **16**, 351 (1970).
10. Hill G.A., James D.J., Ramsden S.A. *Opt. Commun.*, **9**, 237 (1973).
11. Dyer P.E., James D.J. *Appl. Phys. Lett.*, **26**, 331 (1975).
12. Kumar A., Nilaya J.P., Biswas D.J. *Opt. Commun.*, **245**, 289 (2005).
13. Sorochenko V.R., Obraztsova E.D., Rusakov P.S., Rybin M.G. *Kvantovaya Elektron.*, **42**, 907 (2012) [*Quantum Electron.*, **42**, 907 (2012)].
14. Mikhailenko S.N., Babikov Yu.L., Golovko V.F. *Opt. Atmos. Okeana*, **18**, 765 (2005).
15. Prokhorov A.M. (Ed.) *Spravochnik po lazeram* (Handbook of Lasers) (Moscow: Sov. Radio, 1978) Vol. 1, p. 120.
16. Alimpiev S.S. *Dokt. Thesis* (Moscow, General Physics Institute, 1983) pp 24-25.
17. Apollonov V.V., Baitsur G.G., Brytkov V.V., Zienko S.I., Murav'ev S.V., Sorochenko V.R., Firsov K.N., Shakir Yu.A., Yamshchikov V.A. *Pis'ma Zh. Tekh. Fiz.*, **10**, 1192 (1984).
18. Apollonov V.V., Corkum P.B., Taylor R.S., Alcock A.J. *Opt. Lett.*, **5**, 333 (1980).